JTTEE5 16:300–305
DOI: 10.1007/s11666-007-9033-8
1059-9630/$19.00 © ASM International

Peer Reviewed

Deformation of Alumina Droplets on Micro-Patterned Substrates Under Plasma Spraying Conditions

Kentaro Shinoda, Atsushi Yamada, Makoto Kambara, Yoichi Kojima, and Toyonobu Yoshida

(Submitted May 21, 2006; in revised form July 25, 2006)

The deformation of plasma-sprayed alumina droplets of 35-55 μm diameter *d* with an impact velocity of around 90 m/s has been investigated over various micro-patterned substrates with an arithmetic mean roughness of 0.5 μm. On a line-and-space pattern, droplets exhibited elliptical splats extending in the direction perpendicular to the line, when the normalized pattern spacing λ (= *x*/*d*) was 0.1-0.3, where *x* is the pattern spacing. The fingering of the splats was also caused by a concave pattern as well as by a convex pattern and the number of fingers significantly increased at λ = 0.2. In addition, holes suggesting air entrapment were observed off center in the bottom side of each splat by approximately 1.5 times the radius of the droplets, regardless of the pattern. These results suggest the importance of the surface design of substrate on the micrometer scale in plasma spraying.

Keywords diagnostics and control, roughness effects, RF induction plasma spraying, spray deposition

1. Introduction

The deformation of a droplet impinging on a substrate is a critical elemental step in plasma spraying, because it greatly influences the adhesion strength of coatings (Ref 1, 2). On a rough substrate, in particular, the spread dynamics of a droplet could be altered by the roughened structure itself, and heat extraction is also potentially changed by the manner in which the droplet covers the substrate during droplet spread. These could result in air entrapment, fingering, and splashing during droplet spread and also in modified microstructures during solidification.

In practice, grit blasting is applied to the roughening and cleaning of the surface of a substrate to improve coating adhesion mainly by mechanical interlocking. Such treatment has been based mostly on the experience and has several drawbacks. In the case of thermal barrier coatings, for example, thermally grown oxides could be formed preferentially around an uncontrolled rough surface of a bond coat, which degrade adhesion of the top coat during high-temperature operation (Ref 3).

Many studies have shown the correlation of the arithmetic mean roughness R_a with coating properties and adhesion strength, but few experimental studies have shown the correlation of R_a with the deformation of droplets (Ref 4). Stow and Hadfield (Ref 5) showed that R_a is the primary factor for the splashing of water droplets on metal surfaces and that splashing conditions can be determined by the quantity $dV^{1.69}$ when R_a is much smaller than d, where d and V are the diameter and impact velocity of the droplet. Moreau et al. (Ref 6) showed that the apparent degree of flattening and the flattening time of molybdenum droplets on rough surfaces are less than those on smooth surfaces under plasma spraying conditions in the case of glass and molybdenum substrates. Range and Feuillebois (Ref 7) confirmed this tendency using water/glycerin mixtures and substrates with various values of roughness and tried to express it in nondimensional form, i.e., correlating a critical Weber number for splashing with the ratio of d to R_a.

Recently, some researchers have attempted to take account of the shape of surface asperities in conjunction with R_a. Fukanuma (Ref 8) tried to model the surface roughness using several kinds of idealized rough surfaces. Ahmed and Rangel (Ref 9) numerically predicted that splashing would always occur when a droplet impacts an uneven surface, although the degree of splashing changes with R_a and roughness wavelength. Fukumoto et al. (Ref 10) and Cedelle et al. (Ref 11) suggested that the skewness of a rough substrate could affect droplet deformation, even though the case that R_a of their substrate was on the order of several nanometers. Raessi et al. (Ref 12) simulated droplet deformation on a grid pattern substrate in three-dimensional form and suggested that the solidification plays a major role in determining splat shape on a rough surface. These studies suggest that not only R_a but also the shape of asperities play an important role in splat deformation.

Very recently, the deformation of millimeter-sized droplets on a structured surface has been investigated experimentally. Josserand et al. (Ref 13) observed the triggering of a splash by a single-step obstacle and

Kentaro Shinoda, Atsushi Yamada, Makoto Kambara, Yoichi Kojima, and **Toyonobu Yoshida,** Department of Materials Engineering, Graduate School of Engineering, The University of Tokyo, Tokyo, Japan. Contact e-mail: shinoda.kentaro@nims.go.jp.

investigated the angle, speed and dynamics of the liquid sheet emerging as a result of the splash in the case of water droplet on Teflon. Sivakumar et al. (Ref 14) captured the spreading of water drops impinging on structured rough surfaces made of stainless steel and showed that the spread pattern becomes complex with increasing the Weber number. However, no one has attempted to study experimentally such deformation behavior on micro-patterned substrates under plasma spraying conditions.

In this study, therefore, the deformation of an alumina droplet during plasma spraying was investigated on various patterned substrates to study the effect of micropattern on splat morphology.

2. Experimental

Micropatterns were fabricated on quartz glass substrates by photolithography followed by wet etching with buffered hydrofluoric acid (BHF) after rinsing with a standard sulfuric acid/hydrogen peroxide/water mixture. Figure 1 shows the four micropatterns used as substrates in this study: (a) a line-and-space pattern hereafter (L/S), (b) a pillar pattern in a tetragonal array (grid), (c) a pole pattern in a triangular array representative of a convex pattern (obstacle), and (d) a dimple pattern in a triangular array representative of a concave pattern (dimple). While the characteristic depths/heights of these patterns, z, were kept at approximately 1 μm, the areas of concavity and convexity of each pattern were designed to be identical except for the grid pattern. The arithmetic mean roughnesses of these patterns hence corresponded to $R_a = 0.5$ μm. The spacing of these patterns, x, was varied from 4 to 20 μm. Furthermore, in order to clearly observe the deformation of a droplet across the patterns, a smooth surface ($R_a = 0.04$ μm) and a patterned region were aligned alternately. Owing to the isotropic etching of quartz glass by BHF, the edge at the valley bottom becomes rounded with a curvature radius of 1 μm. Although such a slope of the pattern may influence droplet spread, in this study as preliminary analysis, the effect of such a rounded bottom shape was not considered.

Isolated droplet deposition was carried out using a hybrid plasma spray system (Ref 15) with a rotating substrate holder (Ref 16). Fused and crushed alumina powders sieved through a 35-65 μm mesh were injected into hybrid plasma. The experimental conditions are summarized in Table 1. Various micro-patterned substrates were exposed once to a plasma flame on the rotating holder, enabling a consistent spraying of single droplets on all the substrates. Solidified single splats were observed with a laser microscope and a scanning electron microscope. The

Table 1 Experimental conditions

Operating parameter	Value
dc plasma gun	
Ar gas-flow rate, slm	10
Input power, kW	8
rf plasma torch	
Sheath Ar gas-flow rate, slm	50
Sheath H_2 gas-flow rate, slm	1
Input power, kW	40
Carrier Ar gas-flow rate, slm	1
Powder-feeding rate, g/min	1.5
Pressure, Torr	300
Torch-substrate distance, mm	80
Substrate temperature, K	700
Substrate rotation rate, rpm	150

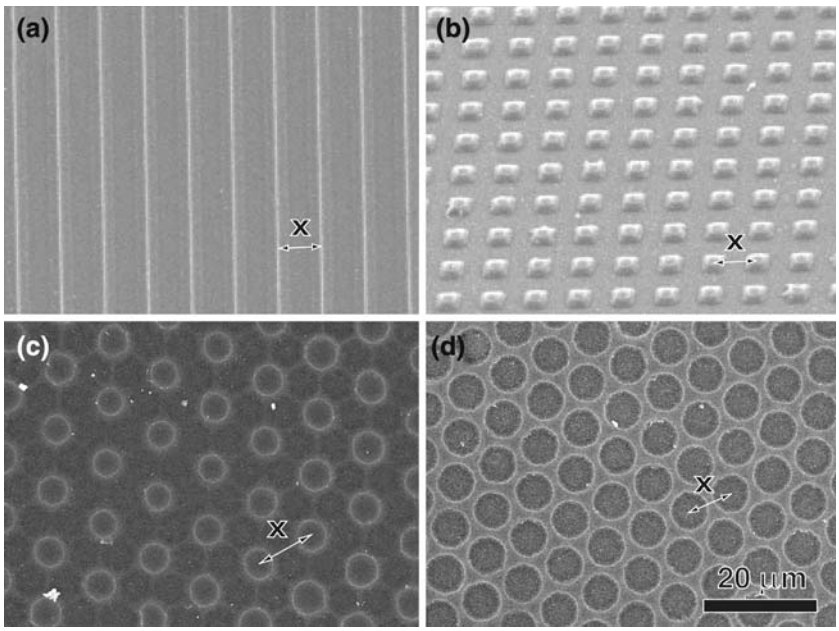

Fig. 1 SEM images of four micropatterns: (a) line-and-space pattern, (b) pillar pattern in tetragonal array, (c) pole pattern in triangular array, (d) dimple pattern in triangular array. The x indicates the pattern spacing for each pattern

droplet diameter was derived from a splat volume. Under these conditions, alumina particles of $d = 35$-55 μm were evaluated to impact on a substrate approximately at V of 90 m/s with a standard deviation of 25 m/s and at temperatures slightly above the melting points of alumina. The velocity was measured by a conventional high-speed camera technique. Hence, the Reynolds number Re and the Weber number We of particles were expected to be around 300 and 2000, respectively.

3. Results

Figure 2 shows the relationship between the splat diameter D and d for splats on a smooth substrate. The gradient indicates the degree of flattening, ξ, which is defined as the ratio of D to d. Under the present deposition conditions, almost all alumina splats exhibited disk shapes, and the average of ξ was 2.8 with a standard deviation σ of 0.2. In this range of interest, the ξ can be then regarded to have no relationship with d. Thus, the effect of surface asperities was discussed within the limitation of this scattering below.

Figure 3(a) shows the optical image of a splat that deformed on a smooth surface across the L/S pattern with $x = 8$ μm. The droplet clearly deformed to have a characteristic nose-shaped splat in the trenched region, whereas it exhibited disk-shaped morphology on a smooth surface. Such unique deformation was evident when the droplet impinged completely onto the trenched surface, as shown in Fig. 3(b). The splat resembled an elliptical shape since the deformation perpendicular to the line patterns was elongated compared with that parallel to the lines. Figure 4 shows the relationship between the normalized pattern spacing λ (= x/d) and ξ on the L/S pattern. Clearly the splat tended to elongate with increasing λ. In particular, it further elongated once $\lambda > 0.1$-0.2, despite the extensive scattering. Note that the depth of the trench was identical among all the patterns, that is, $R_a = 0.5$ μm.

Figure 5(a) and (b) shows optical images of two typical types of splat observed on the grid pattern: one was disk shaped and the other was disk shaped but with fingers. The size and height z of the pillar were 3.6 μm and 1.5 μm, respectively. Figure 5(c) shows the region where splats had fingers on the grid pattern substrate in terms of d and z^* (= z/h), where z^* is normalized pillar

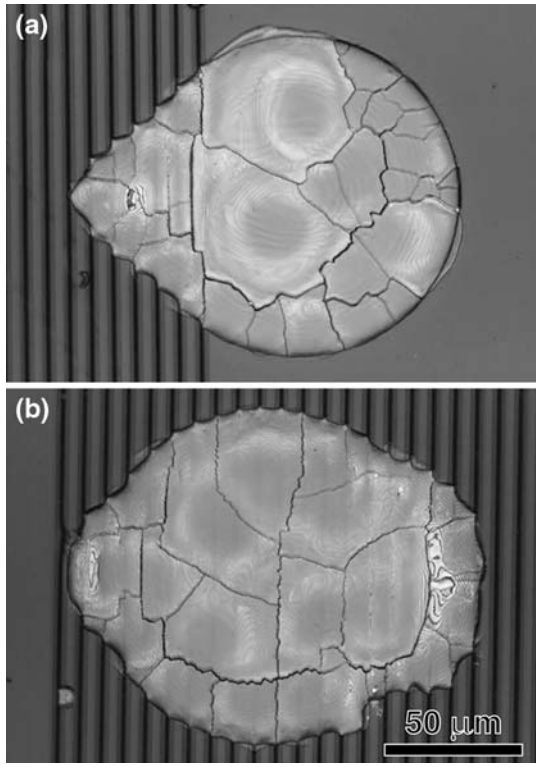

Fig. 3 Laser-microscope images of single splats deforming (a) across the smooth and patterned region and (b) on a patterned region of a substrate. The pattern type is line-and-space whose trench spacing and depth are 8 and 1 μm, respectively

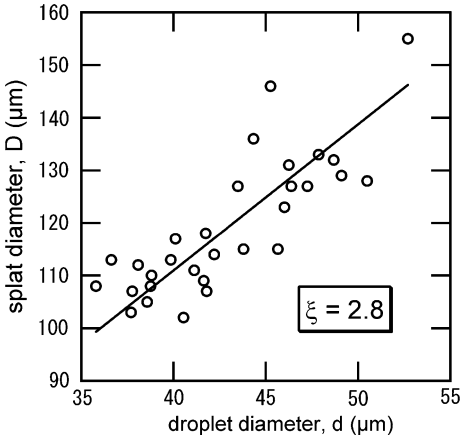

Fig. 2 Relationship between splat diameter D and droplet diameter d. The degree of flattening, ξ, is indicated by a solid line

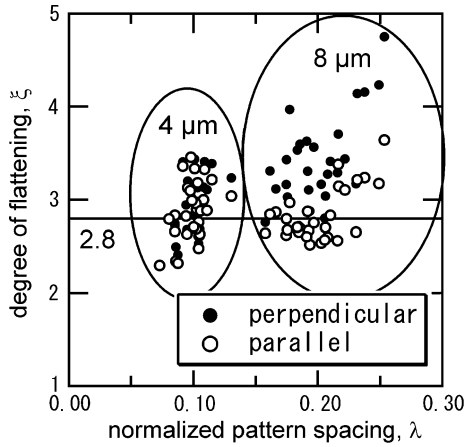

Fig. 4 Relationship between the normalized pattern spacing λ and the degree of flattening, ξ, on L/S-patterned substrate. The pattern spacing of the substrate is 4 or 8 μm

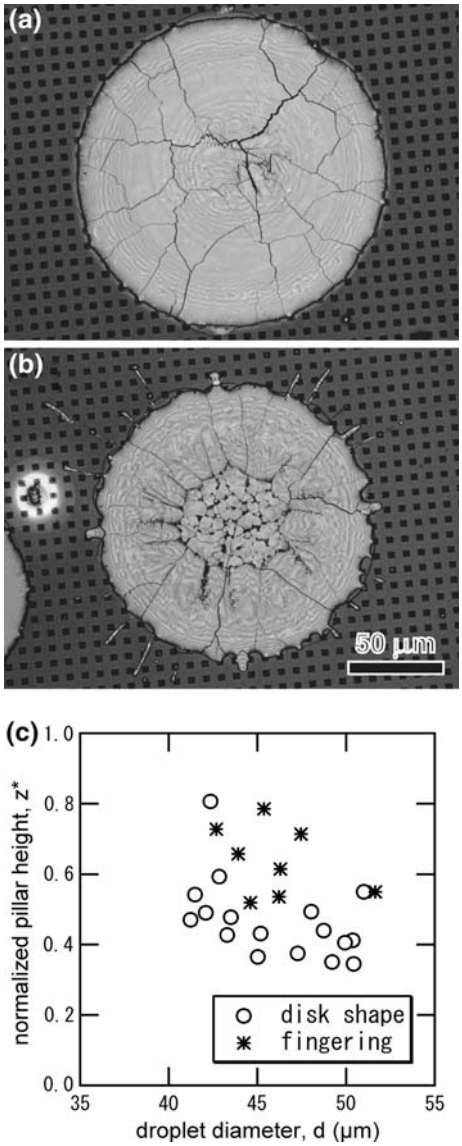

Fig. 5 Laser-microscope images of (a) disk-shaped splat and (b) disk-shaped splat but with fingers on grid-patterned substrate. (c) Distribution of fingered splats

height with splat thickness h. Although fingered splats were observed over the range of d, they existed only where $z^* > 0.5$. Here, we defined "finger" as a finger longer than x. In other words, a small disturbance along the rim of the splat due to the surface pattern was not regarded as a finger. Figure 6 shows the relationship between ξ and d for the splats on the grid pattern and smooth substrate. The average ξ of disk-shaped splats on the grid pattern was 2.8, which was the same as those on smooth substrates, whereas that of fingered splats on the grid pattern was 3.2. Therefore, it can be said that the grid pattern had a weaker effect on the deformation of a droplet unless $z^* > 0.5$.

Figure 7 shows a comparison of splat morphologies on convexo-concave substrates in a trigonal layout of the (a)

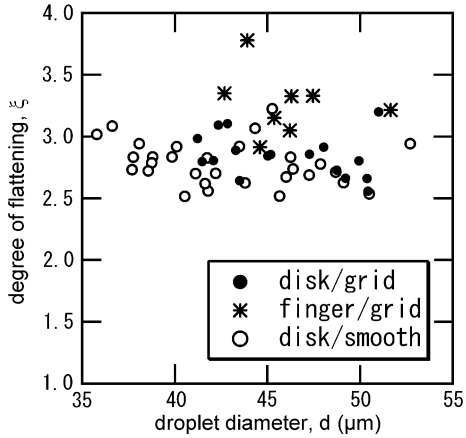

Fig. 6 Variation in the degree of flattening, ξ, with droplet diameter d on a smooth and grid patterned substrate

pole and (b) dimple patterns with a characteristic length of x. It is found in both patterns that droplets deformed fundamentally to disk shapes, and the ξ of the splats was nearly the same as that of the splats on the smooth substrate. However, the distinct features of splats on these substrates are that they exhibited elongation locally in the form of fingering, rather than the characteristic elongation in one direction observed on the L/S pattern. Figure 8 shows the relationships between the number of fingers, N, and λ. The N increased rapidly with increasing λ in the vicinity of $\lambda = 0.1$-0.2, which suggests that a disturbance at the rim of the splat have become large enough to be regarded as fingers at $\lambda = 0.1$-0.2. With a further increase in λ, the N decreased for both substrates, i.e., the substrate roughness tended not to affect splat morphology. Interestingly, the splats on the dimple pattern showed fingering over the wide range of λ as well as those on the obstacle pattern. This suggests that the concave pattern also had a strong effect on splat deformation.

Last, air entrapment by the substrate patterns was observed. Figure 9(a) shows an SEM image of the bottom surface of the coating deposited on the dimple-pattern substrate in the vicinity of the splat center. To observe the bottom surface of the splats, a thick alumina coating was deposited under the same conditions, and the substrate was removed with 50% BHF. Clearly, cavities were formed aligned along the projected periphery of the impinging droplet, as shown by the dotted line. Figure 9(b) shows a summary of the relative positions of the cavities in splats for the various substrate patterns as functions of the characteristic pattern size. Note that cavities were formed at nearly the same relative position within a splat, irrespective of pattern shape, pattern size and its layout, and that their positions were off center by approximately 1.5 the radius of the droplets. Furthermore, from Fig. 9(a), most of the cavities were found to form on the inner side of a dimple, i.e., the edge closer to the splat center.

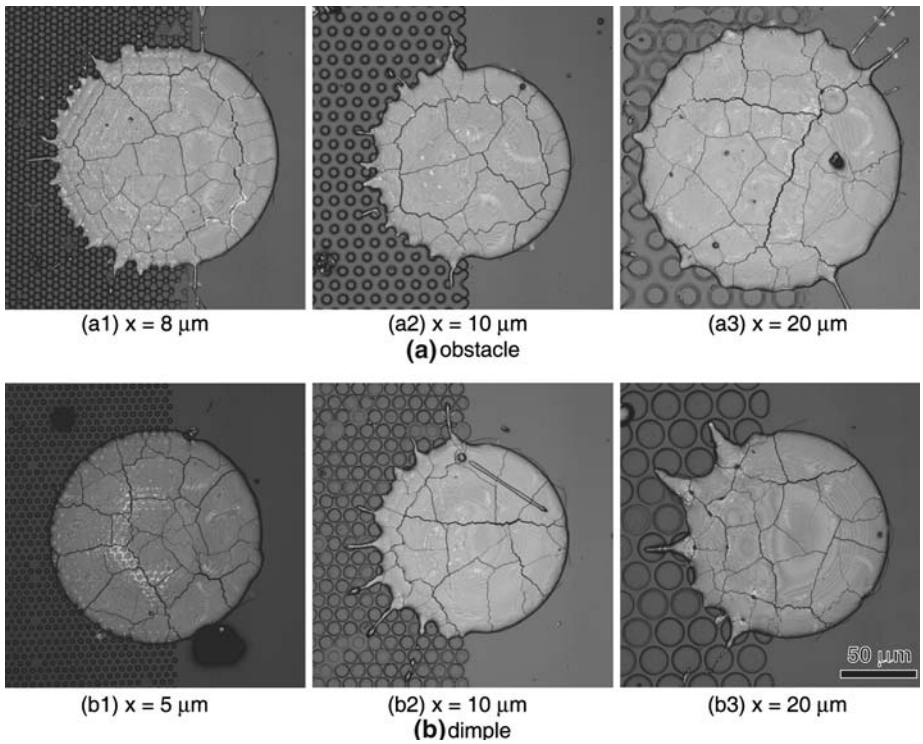

Fig. 7 Laser-microscope images of splats that deformed on (a) obstacle and (b) dimple-pattern substrate with different characteristic pattern sizes x

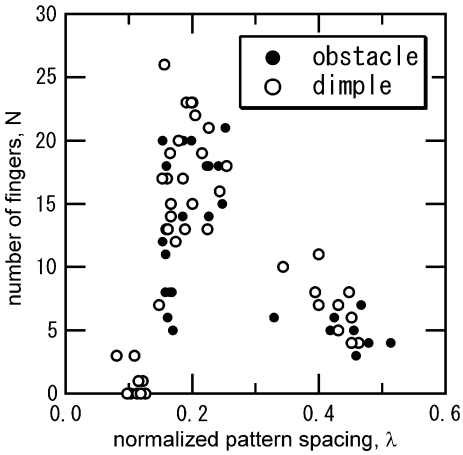

Fig. 8 Relationship between number of fingers, N, and normalized pattern spacing λ (= x/d)

4. Discussion and Conclusions

The anisotropic deformation of molten alumina droplets was observed on various micro-patterned substrates under plasma spraying conditions. Splats elongated in the direction perpendicular to the lines on the L/S pattern, and the degree of elongation tended to increase with the increase in the normalized pattern spacing ranging from 0.1 to 0.3. This is in contrast to the ''static'' spread of a tin droplet on a line-patterned surface with alternating stripe

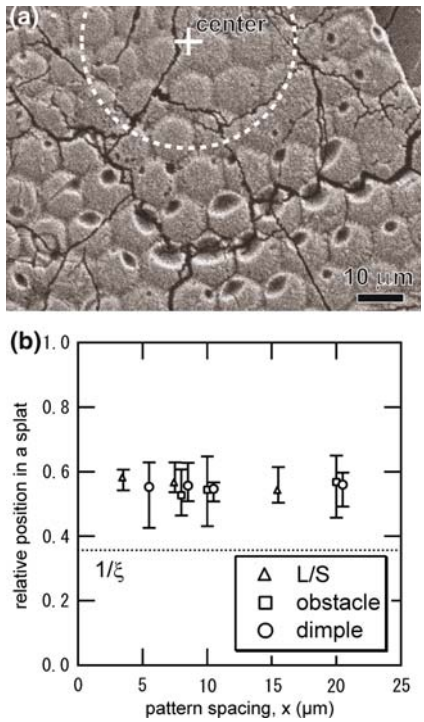

Fig. 9 (a) SEM image of bottom surface of splat that impinged onto 8 μm dimple-pattern substrate. (b) Relative position of air entrapped in splat deposited on various pattern substrates. Null relative position is the center of a splat and $1/\xi$ corresponds to the initial droplet radius. Positions of x of L/S and dimple patterns are shifted to left and right with a 0.5 μm offset, respectively

coatings of different materials in which a droplet elongates in the direction parallel to the lines (Ref 17). In addition, air was entrapped in each splat off-center by 1.5 times the radius of the droplet, regardless of the type, size and pattern layout. Such air entrapment was also observed by Sivakumar et al. (Ref 14) in the case of the impact of a millimeter-sized water droplet whose *Re* is up to 7000. This indicates that the air entrapment in the outer region of a splat on rough substrate is inevitable under plasma spray conditions. These suggest that droplet spread can be affected by a roughness as small as $R_a = 0.5$ μm, indicating the importance of controlling the surface roughness of a substrate on the micrometer scale in plasma spraying.

Our suggestions for designing the surface pattern of a substrate are as follows: First, the size of the surface pattern with a normalized pattern spacing of less than 0.1 would be a favorable pattern for preventing the fingering of splats. Second, convex patterns such as the grid pattern are preferred to concave patterns. Last, the heights of obstacles also influence the fingering of splats. In the case of grid pattern, the heights of pillars less than half the splat thickness will be preferable to reduce the fingering. The critical height of the obstacle for splashing depends not only on spreading lamella thickness but also on the velocity along a horizontal surface (Ref 13), and the threshold of the height will be smaller under dc plasma spraying conditions, whose impact velocities are higher than those observed in this study.

Acknowledgment

The present research was financed by the Japan Society for the Promotion of Science (No. 12305048).

References

1. K. Shinoda, Y. Kojima, and T. Yoshida, In Situ Measurement System for Deformation and Solidification Phenomena of Yttria-Stabilized Zirconia Droplets Impinging on Quartz Glass Substrate Under Plasma Spraying Conditions, *J. Therm. Spray Technol.*, 2005, **14**(4), p 511-517
2. K. Shinoda, T. Koseki, T. Yoshida, Influence of Impact Parameters of Zirconia Droplets on Splat Formation and Morphology in Plasma Spraying, J. Appl. Phys, 2006, **100**(7), Art. No. 074903 (6 pages)
3. N.P. Padture, M. Gell, and E.H. Jordan, Materials Science—Thermal Barrier Coatings for Gas-Turbine Engine Applications, *Science*, 2002, **296**(5566), p 280-284
4. P. Fauchais, M. Fukumoto, A. Vardelle, and M. Vardelle, Knowledge Concerning Splat Formation: An Invited Review, *J. Therm. Spray Technol.*, 2004, **13**(3), p 337-360
5. C.D. Stow and M.G. Hadfield, An Experimental Investigation of Fluid Flow Resulting from the Impact of a Water Drop with an Unyielding Dry Surface, *Proc. R. Soc. Lond. A*, 1981, **373**, p 419-441
6. C. Moreau, P. Gougeon, and M. Lamontagne, Influence of Substrate Preparation on the Flattening and Cooling of Plasma-Sprayed Particles, *J. Therm. Spray Technol.*, 1995, **4**(1), p 25-33
7. K. Range and F. Feuillebois, Influence of Surface Roughness on Liquid Drop Impact, *J. Colloid Interface Sci.*, 1998, **203**, p 16-30
8. H. Fukanuma, Mathematical Modeling of Flattening Process on Rough Surfaces in Thermal Spray, *Thermal Spray: Practical Solutions for Engineering Problems*, C.C. Berndt, Ed., Oct 7-11, 1996 (Cincinnati, OH), ASM International, 1996, p 647-656
9. A.M. Ahmed and R.H. Rangel, Metal Droplet Deposition on Non-Flat Surfaces: Effect of Substrate Morphology, *Int. J. Heat Mass Transf.*, 2002, **45**(5), p 1077-1091
10. M. Fukumoto, M. Ohgitani, and T. Yasui, Effect of Substrate Surface Change on Flattening Behaviour of Thermal Sprayed Particles, *Mater. Trans.*, 2004, **45**(6), p 1869-1873
11. J. Cedelle, M. Vardelle, and P. Fauchais, Influence of Stainless Steel Substrate Preheating on Surface Topography and on Millimeter- and Micrometer-Sized Splat Formation, *Surf. Coat. Technol.*, 2006, **201**(3-4), p 1373-1382
12. A. Raessi, J. Mostaghimi, and M. Bussmann, Effect of Surface Roughness on Splat Shapes in the Plasma Spray Coating Process, *Thin Solid Films*, 2006, **506**, p 133-135
13. C. Josserand, L. Lemoyne, R. Troeger, and S. Zaleski, Droplet Impact on a Dry Surface: Triggering the Splash with a Small Obstacle, *J. Fluid Mech.*, 2005, **524**, p 47-56
14. D. Sivakumar, K. Katagiri, T. Sato, and H. Nishiyama, Spreading Behavior of an Impacting Drop on a Structured Rough Substrate, *Phys. Fluids*, 2005, **17**(10), Art. No. 100608 (10 pages)
15. T. Yoshida, T. Okada, H. Hamatani, and H. Kumaoka, Integrated Fabrication Process for Solid Oxide Fuel Cells Using Novel Plasma Spraying, *Plasma Sources Sci. Technol.*, 1992, **1**(3), p 195-201
16. H. Murakami, T. Yoshida, and K. Akashi, High-Rate Thermal Plasma CVD of SiC, *Adv. Ceram. Mater.*, 1988, **3**(4), p 423-426
17. Y.V. Naidich, R.P. Vorrovich, and V.V. Zabuga, Wetting and Spreading in Heterogeneous Solid Surface-Metal Melt Systems, *J. Colloid Interface Sci.*, 1995, **174**, p 104-111